Proceedings World Geothermal Congress 2023
Beijing, China, October 9 – 11, 2023

Time-lapse Seismic Tomography Analysis for Geothermal Reservoir Characterization During Exploitation Phase within a Liquid-dominated Geothermal Reservoir in Ulubelu Field, Indonesia

Aditya A. Juanda, R.M. Tofan Sastranegara, Mulyanto

Grha Pertamina, Pertamax Tower, 5th floor, Jalan Merdeka Timur No. 11-13. Gambir, Jakarta Pusat 10110

adityajuanda@pertamina.com

Keywords: Microearthquake (MEQ), Velocity, Time-lapse Seismic Tomography, Vp/Vs ratio, Geothermal, Reservoir

ABSTRACT

Microearthquake (MEQ) is a typical geothermal geophysics surveillance method at exploitation phase. The objective of this monitoring technique is primarily to investigate velocity changes within the reservoir for a certain period due to production and injection activities. The MEQ observation in Ulubelu field was carried out continuously using permanent local monitoring network. For a three years period of monitoring, there were recorded over twenty-four thousand P wave and S wave observations from all the recorded earthquakes. The P and S wave onset are hand-picked where the shallow portion of the initial 1D velocity structure derived from sonic log reading from several wells. From the beginning of the observation period, there were additional injection well pads at the southern part due to additional power generations at the field. To monitor the changes of velocity in the vicinity of production and injection wells, travel time seismic tomographic inversions were performed to generate the three-dimensional Vp and Vp⁄Vs structure of the reservoir at each epoch. The ray tracing was calculated using pseudo-bending technique whereas the tomographic parametrization, including grid geometry and damping determination, was tested using the so-called checkerboard resolution test which give a comparable result between all data periods. Based on the tomographic inversion results, an extensive high Vp⁄Vs anomaly from elevation 1 km at the southern part of the field which attributed to the fluids addition from the injection wells. This process may increase Vp by increasing the bulk modulus of rocks while at the same time decreases Vs. The velocity model at the production part was not well resolved due to the MEQ event mostly located in the vicinity of injection well pads. However, subtle low Vp⁄Vs anomaly at the same depth still could be detected at the northern part of the field. To enhance the Vp⁄Vs anomaly, we also construct the relative Vp⁄Vs map (ΔVp⁄Vs) between each epoch. The high ΔVp⁄Vs from each epoch are consistent with the operational and reservoir dynamics of the field. Continuous MEQ surveillance and time-lapse monitoring of Vp, Vs and Vp⁄Vs have a critical contribution in geothermal exploitation phase due to its ability to provide insights of reservoir properties for long term field management.

1. INTRODUCTION

Indonesia is considered to have the world's largest geothermal potentials. PT Pertamina Geothermal Energy (PGE) currently manage 13 contract areas across Indonesia archipelago. Sumatra island has numerous geothermal fields since it hosted abundant volcanoes along the Great Sumatra Fault (GSF) which trends Northwest – Southeast. Previous study (Sieh & Natawidjaja, 2000; Muraoka, et al., 2010) suggests the GSF is defined as dextral slip fault type that interpreted as a highly permeable zone which developed active volcanic arc along the fault lineaments (Figure 1).

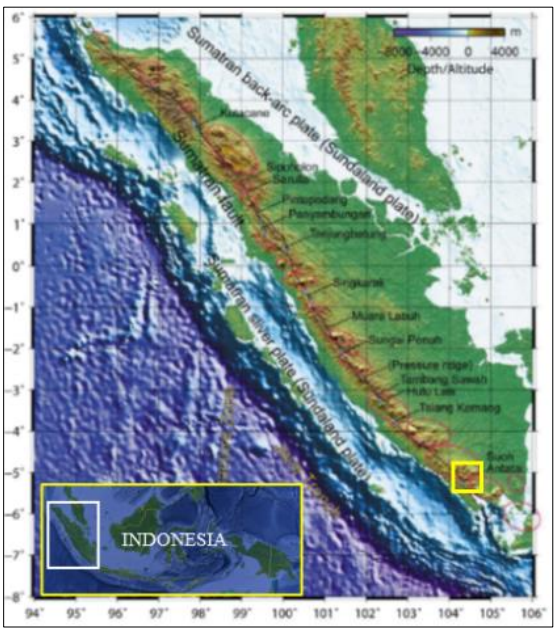

Figure 1 Regional view of the volcanic arc along the Great Sumatran fault (Muraoka, et al., 2010). The Ulubelu field location is indicated by the yellow rectangle shape.

Ulubelu field is a water dominated geothermal field that is situated at the southern tip of Sumatra Island, about 125 km from Bandar Lampung city. Currently, Ulubelu field is generating 220 MW electricity from four power plants unit where the last two power plants, each 55 MW (unit 3 & 4) have been operated from 2016 and 2017, respectively (Purwono & Nugroho, 2021). Microearthquake (MEQ) surveillance was carried out continuously to investigate the local induced seismic distribution within the Ulubelu. After additional injection activities in 2017, time-lapse seismic tomography analysis was conducted to provide insights on how the velocity changes over time within the reservoir.

2. MICROEARTHQUAKE (MEQ) SURVEILLANCE

2.1 MEQ Network Overview

Since 2017, the MEQ network consisting of eight surface geophones has been conducted to monitor seismic activities in the vicinity of Ulubelu field. Each geophone has three-components with 4.5 Hz of natural frequency which is recorded by using the 24-bit SMART-24® series digitizer with 200 samples per second (sps). The production and injection pads in Ulubelu are located well separately at the northern and southern part, respectively (Figure 2) where the injection activity at the most southern part (pad R3 and R4) was started from 2017. The MEQ network covers all the production and injection pads with spacing between sensor around 4 - 5 km.

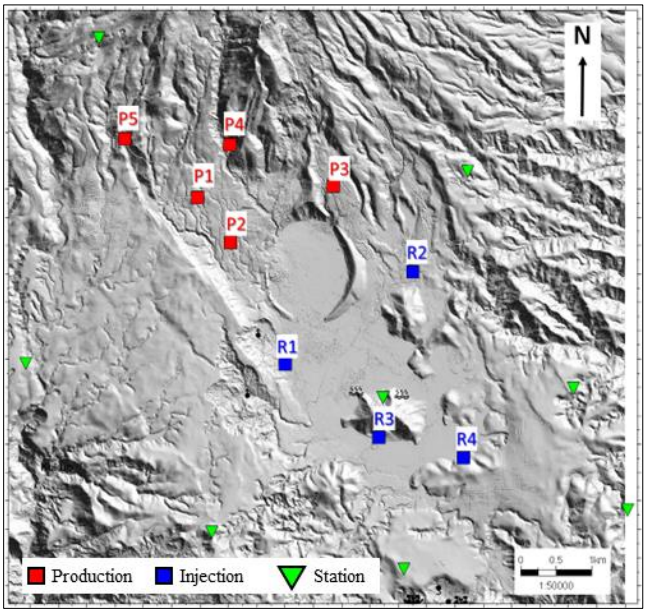

Figure 2 MEQ network in Ulubelu geothermal field. The MEQ station is indicated by green reverse triangle where the production and injection pad indicated by red and blue rectangle, respectively.

2.2 Data

2.2.1 Micro Earthquake (MEQ) Data

Since 2017, the MEQ network consists of eight three-components surface geophones has been conducted to monitor seismic activities in the vicinity of Ulubelu field. There are 22,706 observations of P&S waves from 2017, 2018 and 2019 epochs. Each epoch has a different number of observations as listed in Table 1. The number of observations from 2018 and 2019 epoch is significantly increased from the 2017 epoch due to increasing injection fluids from additional power generation of unit 3 and unit 4.

Table 1. Number of P&S waves observations in each epoch

Epoch	Number of P&S Observations
2017	3,898
2018	8,984
2019	9,824
Total	22,706

The P and S wave arrival times were detected by using an automatic picking routine based on SAPS seismological data acquisition and processing system (Oncescu, et al., 1996) which refined by manual phase picking to validate results. The average spatial error of all the MEQ events is less than 0.35 kilometers.

2.2.2 Velocity Structure

The 1-D layered velocity structure (P-wave and S-wave) used in this study was comprised into two parts (Figure 3, right). The shallower part 1-D layered velocity structure were constructed from sonic log and lithology distribution from wells drilling information, whereas the deeper part was inferred from the generalized earth velocity model namely the Preliminary Reference Earth

Model, PREM (Dziewonski & Anderson, 1981). The Vp⁄Vs ratio used in this study is 1.71 which determined by using Wadati diagram analysis (Figure 3, left).

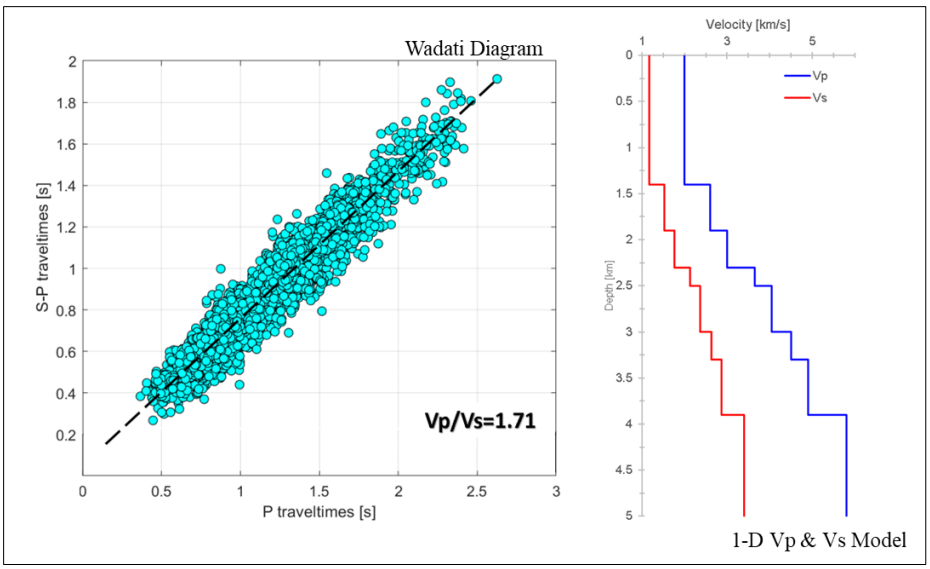

Figure 3 Wadati Diagram (left) and 1-D layered velocity structure (right). The Vp⁄Vs ratio used is 1.71.

2.2.3. Microearthquake (MEQ) Distribution

Based on Figure 4, most of the MEQ events occurred in the vicinity of injection wells (R1, R3, R4) and several production wells which coincide with the major feed zone elevation. Epoch 2017 has the lowest MEQ intensity because it was just the beginning of injection activities at pad R3 and R4 due to additional power generation of 110 MW. Moreover, in epoch 2018 the MEQ intensity in the vicinity of injection pads increased significantly, especially at pad R3 and R4, whereas at pad R1 and R2 the intensity was still within the same range as epoch 2017. Furthermore. In epoch 2019, the MEQ intensity in the vicinity of injection pads relatively decreased relative to epoch 2018. However, there was a distinct MEQ pattern trends NW-SE towards the production pads (P1, P2, P4). This pattern indicates that the subsurface fault or fracture system within the reservoir was reactivated primarily by stress perturbation due to the introduction of injection fluids in the vicinity of production pads as well as fluid withdrawal from producing wells.

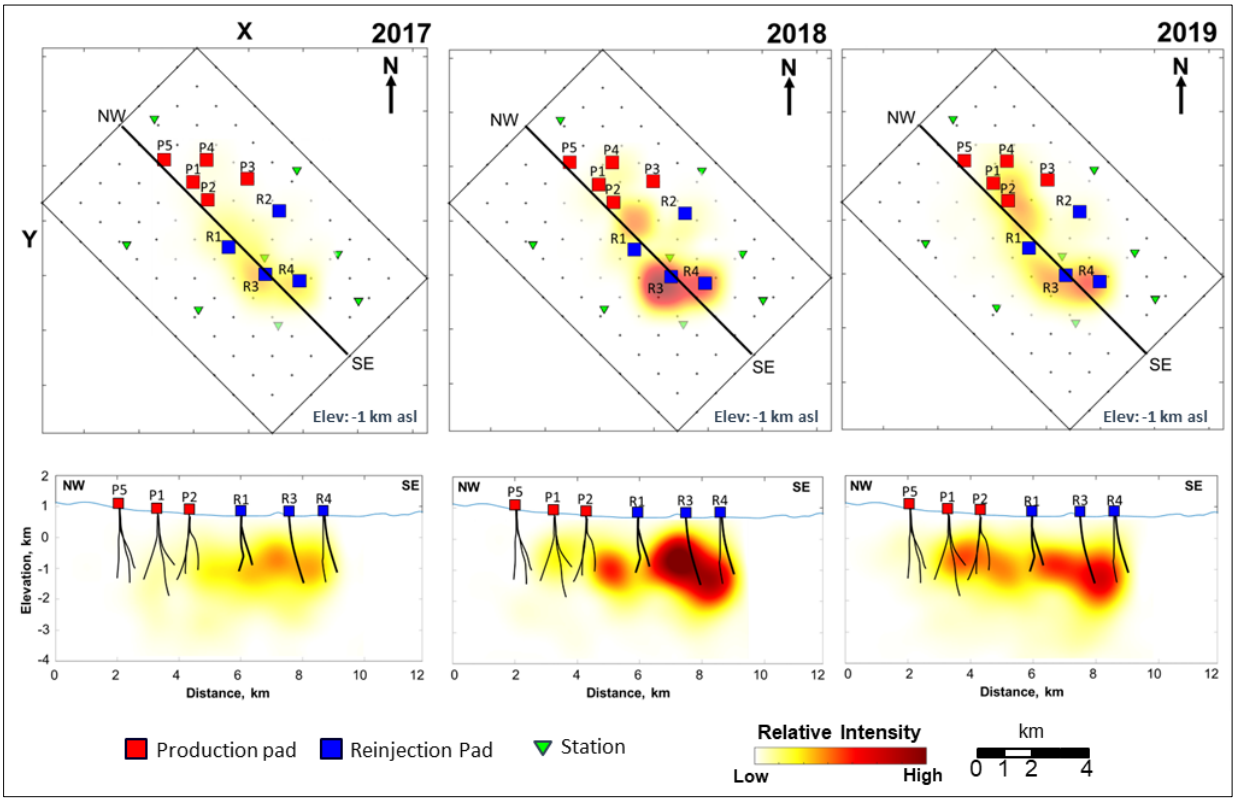

Figure 4 MEQ Events Intensity Map from Epoch 2017, 2018 and 2019. The darker colors indicate higher intensity, most of the MEQ events occurred in the vicinity of injection wells (R1, R3, R4) at elevation -0.5 to -1 km.

3. METHODOLOGY

In order to delineate spatial and temporal velocity changes due to production and injection activities, study of seismic tomography is proposed. Previous studies suggested that seismic tomography technique was successfully construct the velocity structure (Gritto, et al., 2013) and accurately delineate velocity changes within geothermal reservoir (Gunasekera, et al., 2003). In this study, SIMULPS12 program (Evans, et al., 1994) was used in order to do the tomographic inversion, with utilization of PGE's own-developed program to do data and model preparations as well as to visualize the results.

Figure 5 illustrates how the procedures to do the three-dimensional seismic tomography inversion in this study. Based on the workflow, the procedures are divided into three main parts, including Data Preparation, Model Grid Parametrizations, Model Recovery Test and Inverse Modeling. This workflow was implemented on each epoch dataset with the same parameters in order to preserve the model integrity for the time-lapse seismic tomography analysis.

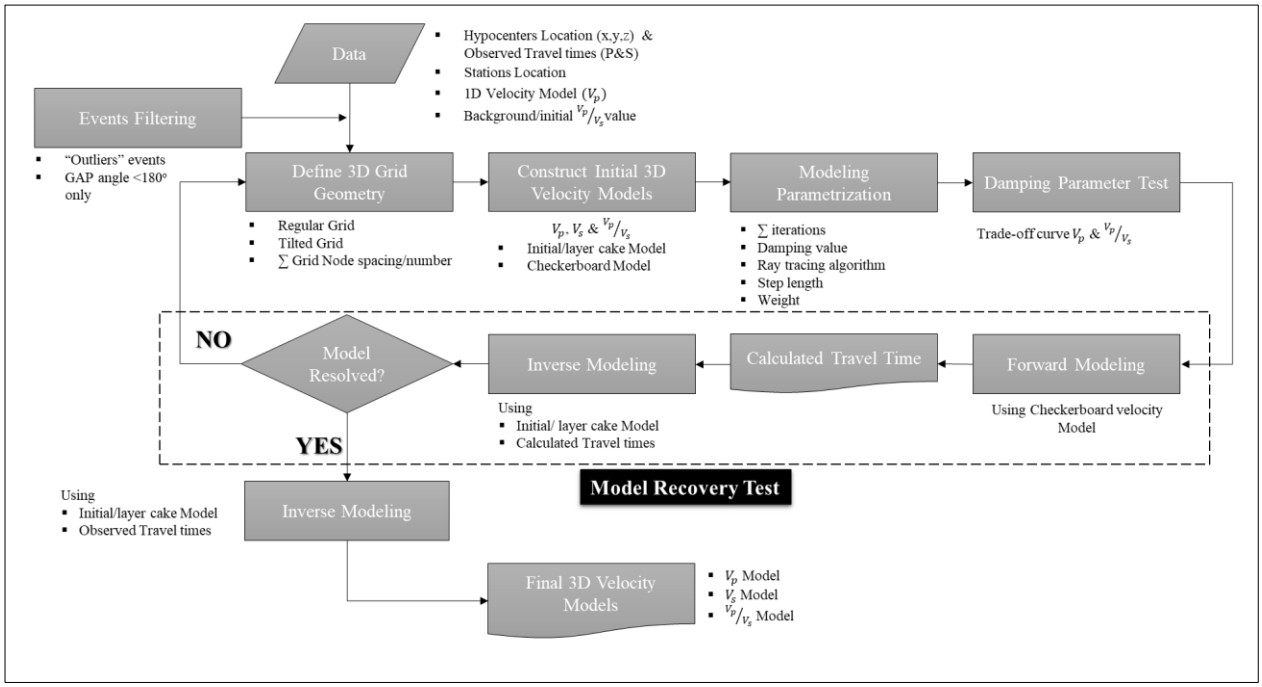

Figure 5 Generalized Three-dimensional Seismic Tomography Inversion Workflow.

3.1 The Data Preparation

This part is to prepare data input, including hypocenter location & observed travel times (P&S), stations location, 1D velocity model of Vp, initial Vp⁄Vs values and to do events filtering. All MEQ data used in this study have an azimuthal gap angle less than 180 degrees or inside the network coverage to minimize the tomographic model uncertainties.

3.2 The Model Grid Parametrizations

This part is to define 3D grid geometry, construct initial 3D velocity models, modeling parametrizations and damping parameter test. The ray tracing algorithm used to do the inversion process is Pseudo-bending Approximate Ray Tracing (Um & Thurber, 1987). The grid is rotated with azimuth N 45° W in order to accommodate MEQ distributions within Ulubelu area (Figure 6). The grid node spacing is a regular 1 kilometer for the Core area whereas the Background area spacing increases gradually which extends to 50 kilometers with total 1650 grid nodes for each Vp and Vp/Vs model. One of the key steps in tomography inversion process is to determine the damping values by using the damping trade-off curves (Figure 7). The appropriate damping value was selected empirically from a series of one-step inversions with different damping values, with a large range of damping values, and plotting data misfit versus model variance (Eberhart-Phillips, 1986). The preferred damping values is on condition to achieve the best compromise between data misfit reduction and model variance (Braeuer, et al., 2012).

3.3 The Model Recovery Test

The purpose of the model recovery test is to assess the ability of the given parameter during tomographic inversion to resolve structural details and to delineates the good resolution area (Figure 8). The first step is to prepare the synthetic checkerboard model with ± 10% perturbation from the initial velocity model and use the model to calculate (forward modeling) P and S wave travel times. The model recovery test is done by doing inversion process using the calculated P and S wave travel times and initial velocity model (layer cake model). Delineation of the good resolution area of each epoch datasets is done by comparing the recovered model to the objective model (checkerboard model), where any inverted cells or grid nodes which can recovers the values of the objective model are considered as the good resolution area. The result of this study suggests that most of the good resolution area from each epoch dataset in the vicinity of the injections section (Figure 9).

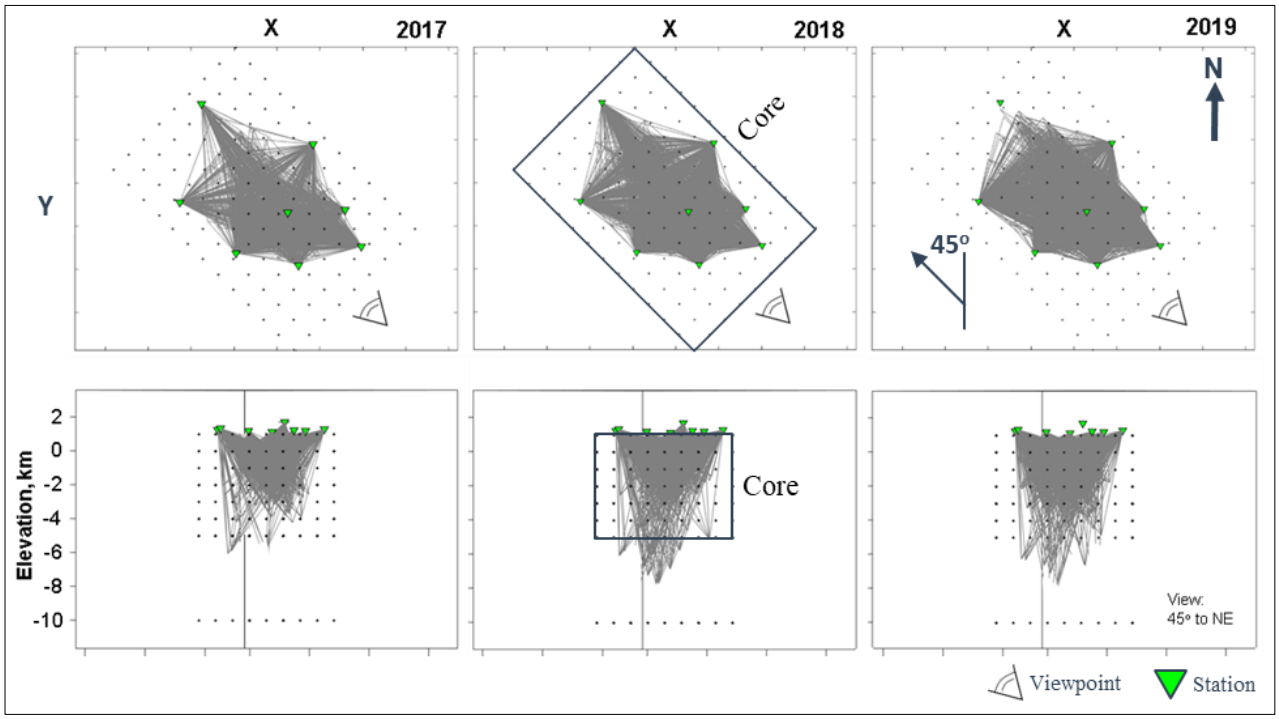

Figure 6 Grid configuration used in tomographic inversion. Note that the grid azimuth is at N 45° W).

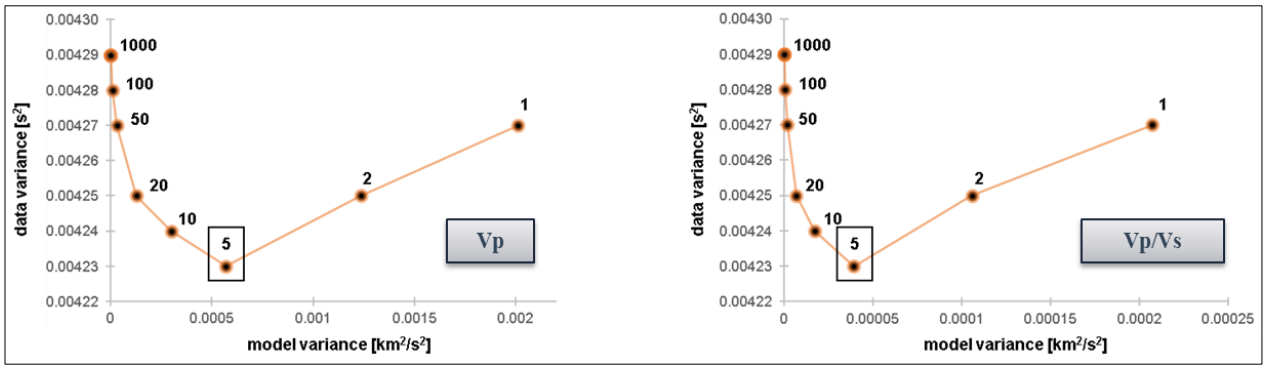

Figure 7 Damping Trade-off Curves. Note that the optimum damping values for Vp and Vp/Vs model.

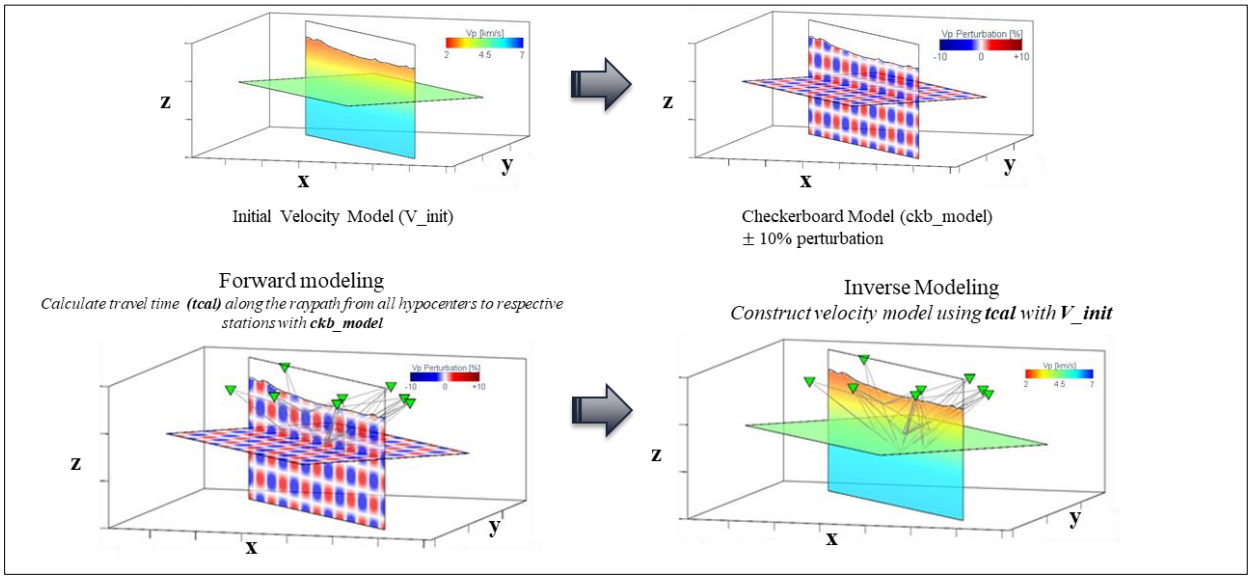

Figure 8 Process of the Model Recovery Test.

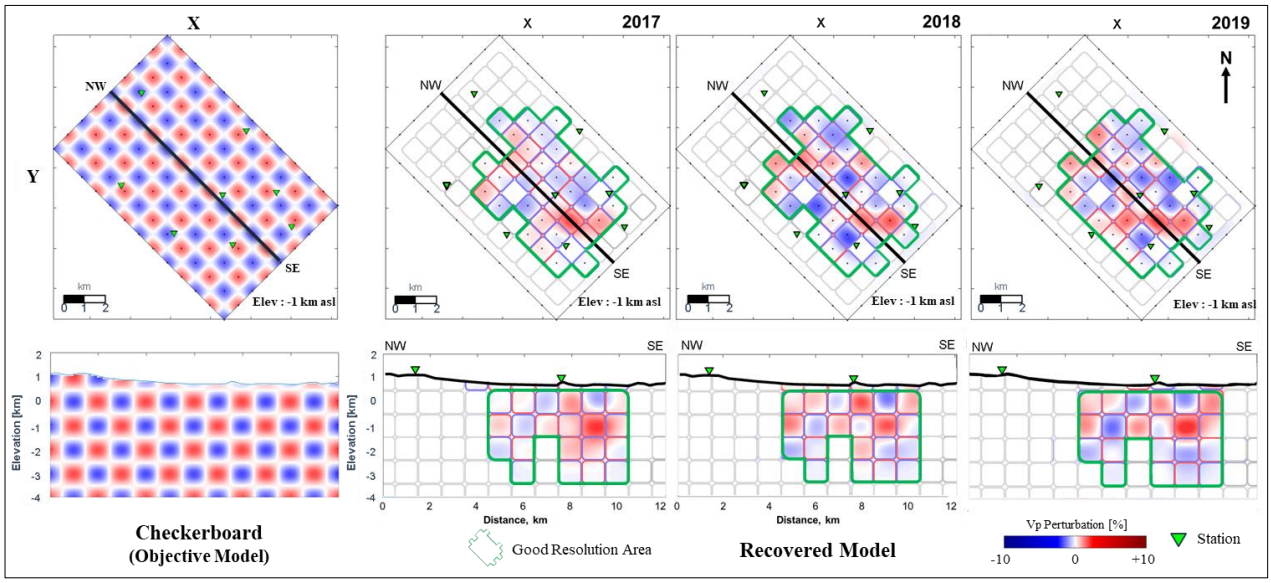

Figure 9 Model recovery test result from epoch 2017, 2018 and 2019. Note that most of the good resolution areas (indicates by the green polygon) are in the vicinity of injection pads.

4. RESULT AND DISCUSSION

Production and injection activities are highly related to local stress field perturbation due to fluid substitutions process which is directly related with fluids contents within the reservoir rocks. In order to map spatial and temporal velocity of the process, analysis of the Vp/Vs ratio is evidently successful. There was an observation of how fractures which saturated by fluids is increasing the Vp/Vs ratio (Moos & Zoback, 1983). On the other hand, a replacement of pore liquid with vapor (steam) within geothermal reservoir would reducing Vp/Vs ratio (Gunasekera, et al., 2003). These observations are consistent with previous study (Boitnott & Kirkpatrick, 1997) which also suggests that high Vp/Vs ratio reflects wet/water phase reservoir whereas low Vp/Vs ratio reflects dry/steam phase reservoir.

4.1 Tomography Inversion Results in Each Epoch

In this study, the tomographic results also suggest consistent results especially at the area with good resolution (Figure 10). In 2017 epoch, high Vp/Vs ratio only occurred in the vicinity R1 injection pad, because at the time almost all the injection fluids from Unit 1 and 2 were injected in R1 pad while at the same time this period is the beginning of injection activities at pad R3 and R4 (not significant changes on Vp/Vs ratio in the vicinity of pad R3 and R4). In 2018 epoch, the Vp/Vs ratio distribution significantly changed, where an extensive high Vp/Vs ratio was observed in the vicinity of pad R1, R3 and R4 as well as penetrating the production area (P1, P2, P3 and P4). Later in the 2019 epoch, the distribution of Vp/Vs ratio across the Ulubelu field was relatively consistent with the previous year with the decreasing magnitude of the Vp/Vs value.

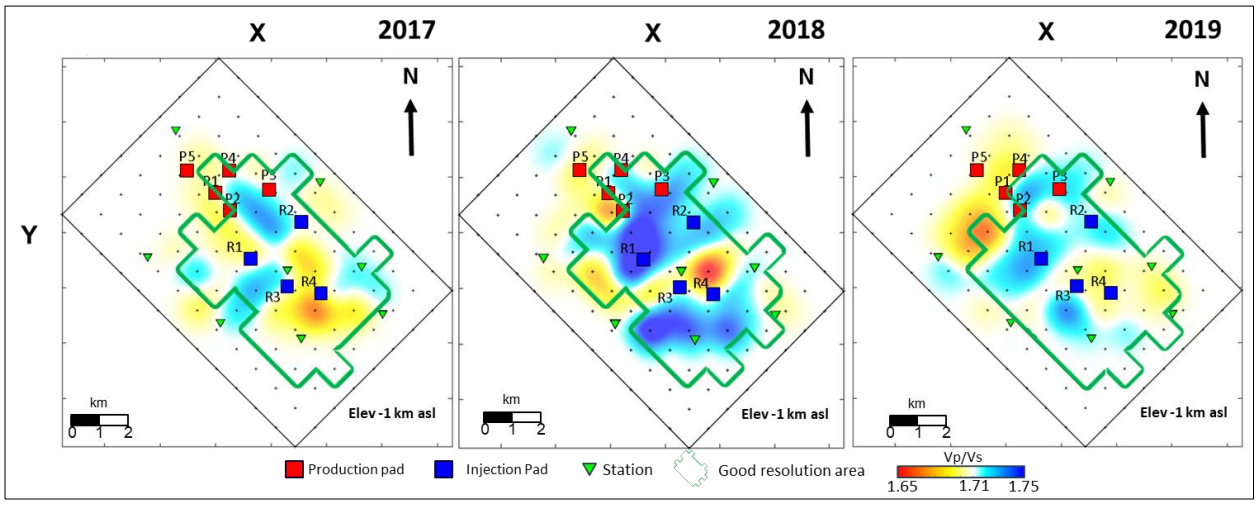

Figure 10 Comparison of Vp/Vs model of epoch 2017, 2018 and 2019 at reservoir level (elevation –1 km). Warm colors indicate low Vp/Vs whereas cool colors indicate high Vp/Vs values.

4.2 Time-lapse Tomography Analysis

In order to enhance the Vp/Vs ratio changes, a time-lapse tomography analysis is implemented. The analysis is simply by subtracting each model with respecting epoch. The warm colors (negative anomaly) indicate reservoir with high temperature and steam saturated condition, whereas the cool colors (positive anomaly) indicate reservoir with low temperature and water or liquid saturated condition. Epoch 2017 is used as the initial conditions relative to Epoch 2018 (called Time-lapse 1), where Epoch 2018 is also used as the initial conditions relative to Epoch 2019 (called Time-lapse 2). This process would produce ΔVp/Vs model Time-lapse 1 and Time-lapse 2 for each epoch, respectively.

Based on Time-lapse 1 model (Figure 11), an extensive & strong positive ΔVp/Vs anomaly (cool colors) trends West – East was observed in at the south direction of injection pads R1, R3 and R4 at major feed zone level (elevation -1 kilometer). These anomalies clearly indicate the presence of cold water and liquid saturated reservoir due to injection activities. There are also observed strong negative Δ Vp/Vs anomaly at elevation -2 kilometers beneath production pads (especially in the vicinity of pad P1 and P2). This indicates the presence of high temperature and steam saturated reservoir although the anomaly is just outside the good resolution area. During Epoch 2018 – 2019 (Figure 12), the distribution of ΔVp/Vs anomalies were changed dramatically. In the vicinity of pad R3 and R4 was observed a weak negative anomaly compared to the 2018 model. This anomaly also co-exists with the positive anomaly beneath production pads. These anomalies might be affected by the fact that the injection water penetrates the production areas which is also supported by the increasing MEQ intensity.

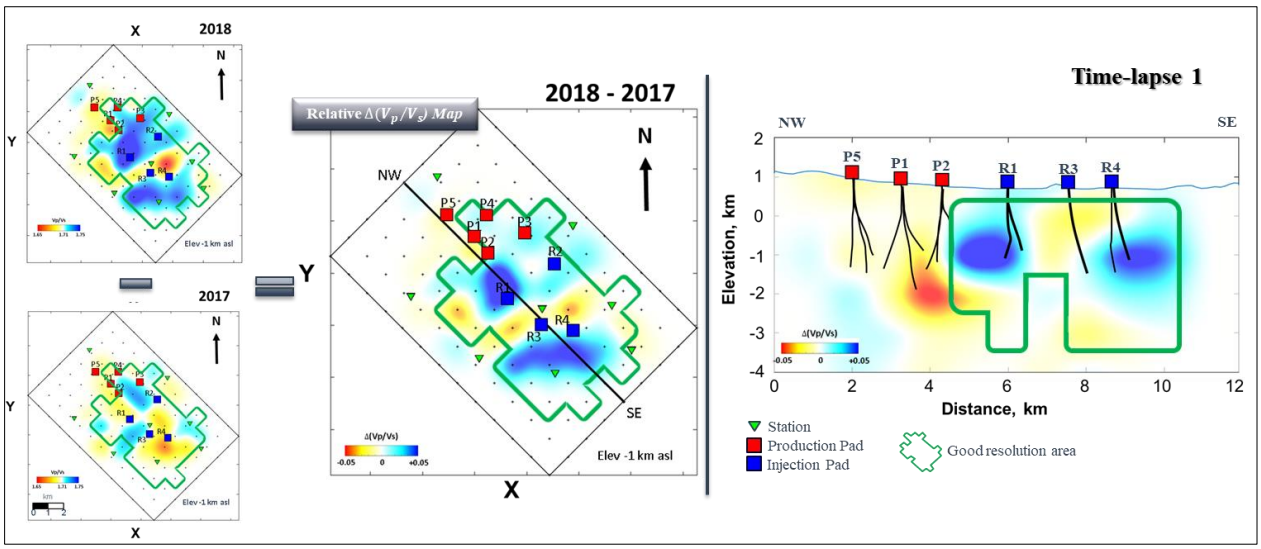

Figure 11 Time-lapse 1 of ΔVp/Vs model. The warm colors indicate steam saturated reservoir whereas the cool colors indicate water saturated reservoir.

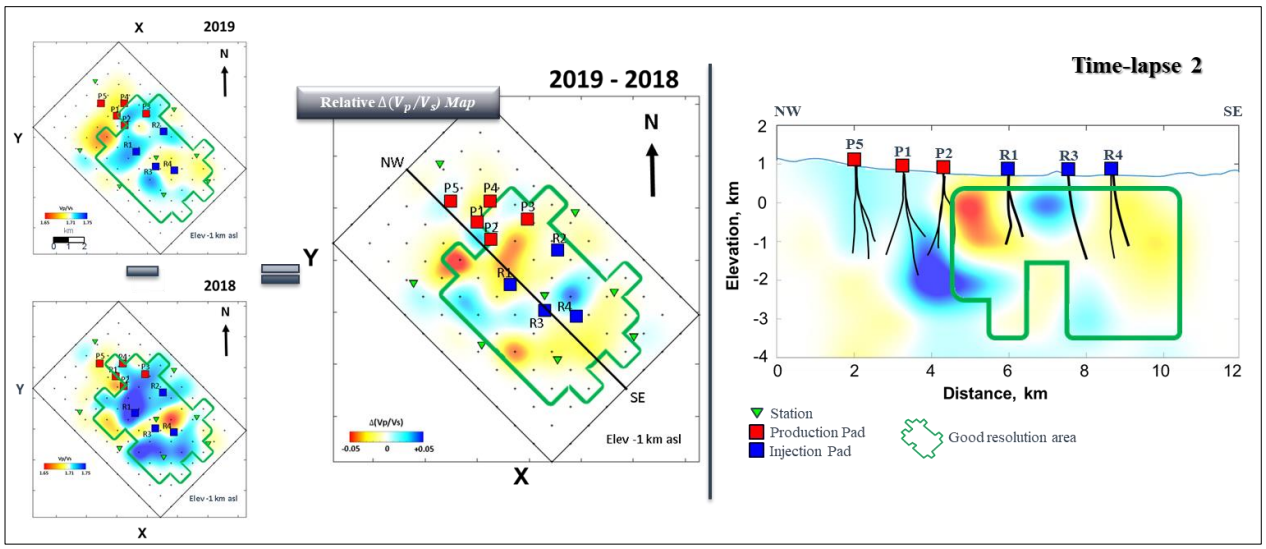

Figure 12 Time-lapse 2 of ΔVp/Vs model. The warm colors indicate steam saturated reservoir whereas the cool colors indicate water saturated reservoir.

5. SUMMARY AND CONCLUSIONS

This study demonstrates the successful applications of time-lapse seismic tomography analysis to characterize fluids content within liquid-dominated geothermal reservoir in Ulubelu field. The results from this study provide insight on how additional injection fluids give distinct and extensive high or positive ΔVp/Vs anomaly in 2018-2017 epoch (Time-lapse 1) where the injection water accumulated in the vicinity of injection pads and flow towards S-SW & SE direction from R3 & R4 and towards N-NW direction from R1. On the other hand, the positive ΔVp/Vs anomaly from 2019-2018 epoch (Time-lapse 2), give an early indication on might be the reinjection fluids flow towards NW direction as confirmed from the event intensity to confirm these results, still need further analysis including from geochemistry and borehole data. Based on the results, seismic tomography analysis could have an important role for reservoir management in geothermal field.

ACKNOWLEDGEMENT

The study presented here was fully supported by Pertamina Geothermal Energy for providing the data, reviewed the manuscript and granted permission to publish this study.

REFERENCES

Boitnott, G. N. & Kirkpatrick, A., 1997. *Interpretation of field seismic tomography at The Geysers geothermal field, California.* Stanford, Twenty-second Workshop on Geothermal Reservoir Engineering.

Braeuer, B. et al., 2012. High-resolution local earthquake tomography of the southern. *Geophysical Journal International,* Volume 191, p. 881–897.

Dziewonski, A. M. & Anderson, D. L., 1981. Preliminary reference Earth model. *Physics of the Earth and Planetary Interiors,* pp. 25(4), 297–356.

Eberhart-Phillips, D., 1986. Three-dimensional velocity structure in northern California Coast Ranges from inversion of local earthquake arrival times. *Bulletin of the Seismological Society of America.*

Evans, J. R., Eberhart-Phillips, D. & Thurber, C. H., 1994. *User's manual for SIMULPS12 for imaging Vp and Vp/Vs: A derivative of the Thurber tomographic inversion SIMUL3 for local earthquakes and explosions,* s.l.: U.S. Geological Survey.

Gritto, R., Yoo, S.-H. & Jarpe, S. P., 2013. *Three-dimensional Seismic Tomography at the Geysers Geothermal Field, CA, USA.* Stanford, Thirty-Eight Workshop on Geothermal Reservoir Engineering.

Gunasekera, R., Foulger, G. R. & Julian, B. R., 2003. Reservoir depletion at The Geysers geothermal area, California, shown by four-dimensional seismic tomography. *Journal of Geophysical Research.*

Moos, D. & Zoback, M. D., 1983. In situ studies of velocity in fractured crystalline rocks. *Journal of Geophysical Research,* Volume 88, p. 2345– 2358.

Muraoka, H. et al., 2010. *Geothermal Systems Constrained by the Sumatran Fault and Its Pull-Apart Basins in Sumatra, Western Indonesia.* Bali, s.n.

Oncescu, M. C., Rizescu, M. & Bonjer, K. P., 1996. An Automated and Networked Seismological Acquisition and Processing System. *Comput Geosci,* pp. 22 (1), 89–97.

Purwono, N. & Nugroho, A. J., 2021. *The Development of Ulubelu Geothermal Power Plant 2x55 MW - Lampung Indonesia.* Reykjavik, s.n.

Sieh, K. & Natawidjaja, D., 2000. Neotectonics of The Sumatran Fault, Indonesia. *Journal of Geophysical Research Vol. 10,* pp. 28,295 - 28,326.

Um, J. & Thurber, C., 1987. A fast algorithm for two-point seismic ray tracing. *Bulletin of the Seismological Society of America,* Volume 77, p. 972–986.